American Mineralogist, Volume 109, pages 2–7, 2024

Crystal growth according to the law of proportionate effect

D.D. Eberl[1,*]

[1]Retired from the U.S. Geological Survey

Abstract

This paper summarizes an approach to crystal growth that was published in parts in various articles over the course of 25 years by the present author and his colleagues. Evidence for this approach, which is confirmed in detail by data in the cited publications and in the figures and equations in the supplementary material that accompanies this paper (see the Online Materials[1]), comes mainly from the shapes of crystal size distributions (CSDs). Such distributions reveal the growth histories of natural minerals and synthetic compounds, histories that can be used to make geological interpretations and to guide industrial syntheses.

CSDs have three fundamental shapes: log-normal, asymptotic, and Ostwald. These shapes result from different degrees of supersaturation near the time of nucleation. The first two distribution shapes form according to the Law of Proportionate Effect (LPE) at moderate supersaturation, and the latter rare distribution forms by Ostwald ripening at large supersaturation. Initially, the first two distributions have mean diameters of up to tens of nanometers and grow by surface-limited growth kinetics. The slow step in this reaction is the incorporation of nanoparticles (bits of crystal or adparticles) onto the crystal surface. As the crystals become larger, their demand for nutrients, as calculated by the LPE, increases exponentially. Then the slow step in the reaction changes to the rate of transfer of nutrients to the crystal (supply- or transport-limited growth). Crystal diameters often grow the most during this latter stage, and the initial CSD shapes that originally formed during surface-limited growth are retained and scaled up proportionately.

Proportionate growth during the supply-limited stage can be simulated approximately by multiplying the diameter of each crystal in a distribution by a constant. Crystals can also grow by a constant rate law in which a constant length is added to each crystal diameter in the distribution. This rare process causes the original CSD to narrow so that its initial shape is not preserved. The growth law that prevails, either proportionate or constant, is determined by the manner in which nutrients are supplied to the crystal. Supply is by advective flow during proportionate growth, with the nutrient solution moving with respect to the crystals. Constant growth relies on the random diffusion of nutrients through a quiescent solution. Proportionate growth is by far the most common growth law, and therefore, nutrient supply by diffusion alone during crystal growth is uncommon.

Distributions formed by Oswald ripening and those formed by other rare processes are also discussed. During Ostwald ripening, nucleation caused by mixing reactants at large supersaturation forms crystals that are extremely fine and numerous. The larger crystals grow at the expense of the finer, less stable crystals, thereby forming, on completion, the universal steady-state CSD shape predicted by the Lifshitz-Slyozov-Wagner (LSW) theory. This unique CSD shape, as well as other rare shapes, then are scaled up to larger sizes by supply limited proportionate growth.

Keywords: Crystal growth, proportionate growth, constant growth, Ostwald ripening, crystal size distributions, Law of Proportionate Effect, crystallization, nucleation, stochastic crystal growth

Growth of log-normal crystal size distributions

Minerals most commonly have log-normal crystal size distributions [CSDs; Figs. 1, 15, and 17 in Eberl et al. (1998); Fig. 2 in Kile and Eberl (1999); Figs. 3 and 9 in Kile et al. (2000); Fig. 5b in Bove et al. (2002); Figs. 1 and 3 in Eberl et al. (2002a); Fig. 3 in Kile and Eberl (2003); Figs. 5 and 7 in Badino et al. (2009); Fig. 3 in Eberl (2022)]. A log-normal distribution (Fig. 1) is described by the equation:

$$g(X) = \left[\frac{1}{X\beta\sqrt{2\pi}}\right]\exp\left\{-\left(\frac{1}{2\beta^2}\right)\left[\ln(X)-\alpha\right]^2\right\} \quad (1)$$

where $g(X)$ is the continuous theoretical frequency distribution of variable X, where, in this case, the Xs are crystal diameters that are parallel to a given crystallographic direction. Equation 1 can be solved if two parameters are known: α and β^2 are the mean and variance of the distribution of the natural logs of X. The original scale units for α need to be specified because it is a log. β^2 indicates the breadth of a distribution for a given α.

* E-mail: ddeberl@gmail.com

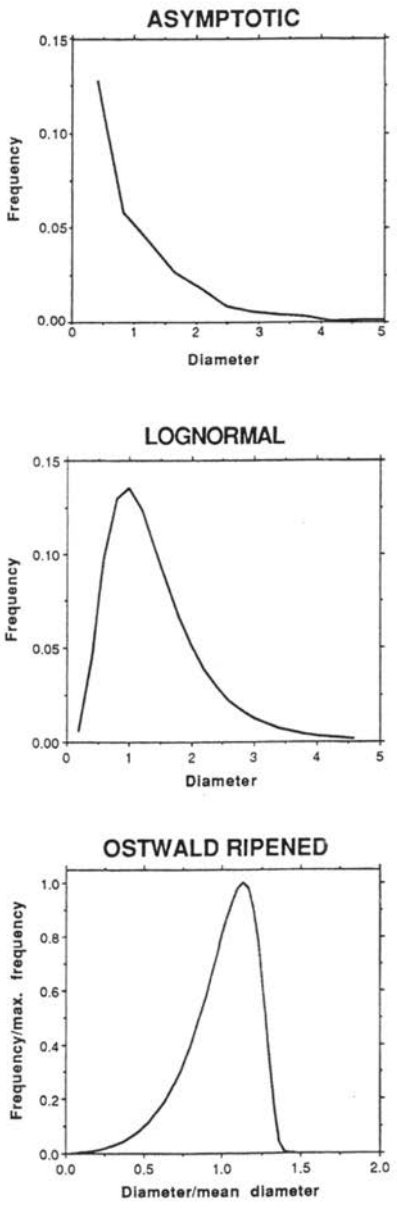

Figure 1. The three fundamental shapes for crystal size distributions. All have been produced in synthesis experiments, by calculation, and have been found in nature. This figure is from Kile et al. (2000).

Iteration of the Law of Proportionate Effect (LPE) is the simple mathematical procedure that generates the log-normal distribution (Koch 1966) and thereby simulates crystal growth (Eberl et al. 2000):

$$X_{j+1} = X_j + \varepsilon_j X_j \quad (2)$$

where X_j is the diameter of an individual crystal, ε_j is a random number that varies independently for each crystal between 0 and 1, and j denotes the calculation cycle for the LPE iteration. Starting, for example, with 1000 crystals having a diameter of 1 nm, Equation 2 is solved j times for each crystal by substituting X_{j+1} back into the equation for X_j. The distribution evolves from an even distribution into a log-normal one when the crystal sizes resulting from the LPE calculation are grouped into equally spaced bin sizes, using the bin centers as X. For example, sizes calculated by the LPE that range between 2.5 and 3.5 nm are grouped as 3 nm, and the number of crystals in the bin is noted. Continued iteration of the LPE leads to an increase in the mean size and variance of the distribution [Fig. 2 in Eberl et al. (1998)].

The results of the LPE calculation are verified as being log-normal by calculating the parameters α and β^2 from the numbers of crystals in the binned LPE sizes, where $\alpha = \Sigma \ln(X) f(X)$, and $\beta^2 = \Sigma[\ln(X) - \alpha]^2 f(X)$, where $f(X)$ is the frequencies of binned crystal sizes X. The two parameters are entered into Equation 1, and the theoretical log-normal number of crystals for each binned size is calculated from Equation 1 by multiplying a normalized $g(X)$ times the total number of crystals counted, in this case 1000. This distribution is compared statistically (using the Chi-square test or the Kolmogorov-Smirnov test for sparse data) to the distribution of crystals calculated from the LPE to verify the log-normal shape. The same general procedure is used to test measured distributions for log-normality.

The LPE is assumed to be the central equation that describes relative crystal growth rates in natural and synthetic systems because it duplicates the experimentally measured log-normal shapes of natural and synthetic CSDs (Eberl et al. 1998, 2002a). The LPE models crystal growth as a stochastic process, as opposed to being deterministic. This means that although crystal growth has a random component (ε), this randomness follows a rule (the LPE). Therefore, although the relative growth rates of individual crystals cannot be calculated precisely, the distribution shape calculated by iterating Equation 2 is predictably log-normal.

If the LPE is taken literally, it offers other insights into the growth process. The growth particles (termed nanoparticles, adparticles, or colloids) that attach themselves to a crystal's surface are a random fraction of a crystal's initial size ($\varepsilon_j X_j$) rather than being individual atoms, ions, or monomers. Such crystallization by oriented particle attachment is supported by electron micrographs that show diverse types of nanoparticles in various stages of attachment [e.g., Fig. 12 in Ivanov et al. (2014); Fig. 2 in De Yoreo et al. (2015)]. Atom by atom or molecule by molecule growth would not produce log-normal CSDs. Also, according to the LPE, growth by the coalescence of nanoparticles occurs in discrete cycles (j) rather than continuously.

The LPE also indicates that the relative rate of crystal growth is a function of the linear dimensions of the crystal (i.e., of its diameter X) rather than of its surface area or volume. In the older literature, this type of growth was termed size-dependent growth, but more specifically, it is now termed proportionate growth. Whereas previously such growth was considered to be a rarity, proportionate growth is, in fact, the most common growth mechanism (Eberl et al. 1998). The random variable in the LPE also clarifies crystal growth dispersion, whereby individual crystals, all initially of the same size and each subjected to identical growth environments, can grow at different rates [see Eberl et al. (1998) p. 503, for pertinent references].

The LPE (Eq. 2) is not the complete story because the pre-

dicted growth rate cannot be sustained. Unconstrained iteration of the LPE leads to exponential growth and eventually to very large adparticles and distribution variances [Figs. 2 and 3 in Eberl et al. (1998)]. However, Equation 2 applies only to the initial stages of growth, immediately during and after nucleation, when calculation of the growth rate is limited only by the incorporation of nanoparticles ($\varepsilon_j X_j$) onto the crystal surface. It is a rate that prevails at distribution mean sizes that range up to tens of nanometers [as indicated by Fig. 2 in Eberl et al. (1998)]. At larger sizes, calculation of the growth rate is limited by the rate of supply of material to the crystal rather than by incorporation onto the surface. Equation 2 is modified for supply limited growth to account for a limited volume of nutrients carried to the surfaces during each calculation cycle (j) of the LPE (for details concerning this volume-limiting calculation, see Eq. 8 in Eberl et al. 1998, or Eq. 2 in Kile et al. 2000). This modification of the LPE leads to the calculation of adparticles that are limited in size, that are small compared to the size of the growing crystal, and that preserve β^2 during growth. Thus surface-limited growth initially gives the distribution a log-normal shape, whereas subsequent supply-limited growth preserves this shape (meaning that β^2 remains constant) as the mean size (α) increases [see Fig. 6 in Eberl et al. (1998); Fig. 7 and Table 2 for continuous growth experiments in Kile et al. (2000); see Fig. 3 for a similar experiment in Eberl et al. (2002a)].

The growth of a distribution during supply-limited growth can be duplicated approximately by multiplying the crystal sizes in the distribution by a constant (k, which is a constant of proportionality or scale factor). Equation 2 then reduces to $X_{(j+1)} = kX_j$, where the constant k substitutes for the random variable $(1 + \varepsilon_j)$. This procedure increases the distribution's mean size while keeping its variance constant. However, this calculation, although convenient, is not completely satisfactory because multiplication by k does not express the random tendency for growth found at small diameters. Multiplication by k causes the growth rate of individual crystals to be predictable. A more realistic calculation applies the volume-adjusted growth limit for each iteration of the LPE, as was discussed above. The shape of the resulting distribution is the same for either calculation, but the sizes of individual crystals differ because the latter calculation contains a random number rather than a constant [Fig. 2b in Eberl et al. (2002a)].

CSDs that have very different mean sizes, ranging from nanometers [e.g., illite crystal thicknesses; see Fig. 5b in Bove et al. (2002)] to meters [giant gypsum crystals in Naica's Cueva de los Cristales that range to >11 m long; see Figs. 5 and 7 in Badino (2009)], have log-normal shapes with similar variances [e.g., Fig. 16 in Eberl et al. (1998) and Fig. 7 in Kile et al. (2000)]. Such shapes most likely result from the proportionate growth of log-normal distributions that were formed according to LPE growth early in crystallization. Other growth mechanisms, such as ripening, constant growth or entirely random growth, would quickly destroy the log-normal shape and alter the variances [Fig. 8 in Eberl et al. (1998); Figs. 2 and 3 in Eberl et al. (2002a)]. Therefore, control of the initial CSD shape during and immediately after nucleation is key to controlling the shape of the final CSD because the earlier shape is scaled up during supply-limited growth.

Formation of CSD shapes other than log-normal

Diverse conditions near the time of nucleation can lead to various CSD shapes. These shapes include the commonly found asymptotic CSD and the rare Ostwald, transitional, non-Ostwald, and multimodal CSDs.

Nucleation occurs in supersaturated solutions when crystals appear that have radii (r) greater than that of the critical radius (r*). If $r > r^*$, crystals can nucleate and grow. If $r < r^*$ then they dissolve. A crystal having a size equal to r* is in equilibrium with the solution and neither grows nor dissolves. A solution needs to be supersaturated, rather than simply saturated, to form growing nuclei because the saturation state for a mineral (i.e., its solubility product) is determined for the infinitely large crystal and, therefore, does not address an increase in solubility related to an increase in specific surface energy for finer crystals. Furthermore, concentrations measured for a bulk solution do not address inhomogeneities present in a solution at the nanometer scale (particularly upon mixing), further complicating the calculation of r*. In addition, the value for r* may increase during nucleation and growth if the saturation level falls as crystallization proceeds.

Experiments with calcite nucleation and growth and with computer simulation (Eberl et al. 1998, 2000; Kile et al. 2000) indicate that variations in nucleation history can lead to CSD shapes that are not log-normal. For example, if nucleation occurs over an extended time at a constant or accelerating nucleation rate while previously formed nuclei grow according to the LPE, an asymptotic distribution (Fig. 1) results in which the smallest size category has the largest frequency [see also: Table 2 and Figs. 4 and 13 in Eberl et al. (1998); Fig. 2 in Kile et al. (2000)]. After an initial period of nucleation and growth, this shape can be preserved (β^2 is held constant) and scaled up by subsequent supply limited proportionate growth, as was discussed. This commonly occurring asymptotic shape can be described approximately using the log-normal equation (Eq. 1), but it does not often pass the statistical test. It can readily evolve into a log-normal shape if nucleation ceases while surface-limited growth continues [Figs. 6 and 7 in Bove et al. (2002)].

A second complication in CSD shape is related to nucleation that occurs when concentrated solutions are suddenly mixed. Such an event, which is rare in nature, can lead to the universal steady-state shape that is expected for supply-limited Ostwald ripening, a distribution that is skewed opposite to that of log-normal (Fig. 1). The equation for this shape was derived independently by Lifshitz and Slyozov (1961) and by Wagner (1961) in what is known as the LSW theory. As was similarly discussed for the log-normal distribution, the LSW equation that describes the Ostwald distribution (Eq. A20 in Eberl et al. 1998) differs from the simple equation that is iterated to simulate the distribution (Eq. 10 in Eberl et al. 1998, presented by Markworth 1970). Experiments and calculations (Kile et al. 2000) have shown that this unique universal steady-state shape forms initially at very large levels of supersaturation, where abundant and extremely fine nuclei precipitate. A large contrast in specific surface areas among these particles leads to the growth of the larger nuclei ($r > r^*$) at the expense of the dissolution or the incorporation of the smaller, less stable nuclei ($r < r^*$) according to the Ostwald ripening mechanism, with r* approximated by the mean radius.

According to LSW theory, the CSD for any mineral that has undergone sufficient ripening will have the identical negatively skewed distribution shape when the data are plotted on reduced axes (size/mean size vs. frequency/maximum frequency), a shape that is independent from the initial, pre-ripened CSD shape, and that has a cutoff at large sizes [Fig. 1; see also Fig. 4 in Kile et al. (2000)]. The coincidence of CSDs on a reduced plot means that the variances are equal. The Ostwald shape, which has a constant and small variance of about 0.06, is scaled up by supply-limited growth, which leads to an increase in mean size while the variance is preserved. The resulting crystals all have nearly the same size [Fig. 8 in Kile et al. (2000)].

The Ostwald CSD forms initially at large supersaturation, whereas the log-normal shape forms initially at smaller supersaturation. Nuclei precipitated at smaller saturation are larger and fewer and, therefore, are less subject to ripening. Calcite crystallization experiments [Table 1 and Fig. 6 in Kile et al. (2000)] showed that log-normal CSDs formed at initial omegas ranging from 22 to 40, where omega is defined as the ion activity product of the solution divided by the mineral solubility product. Therefore a solution with an omega of one is at equilibrium with a crystal that has negligible specific surface energy. However, the Ostwald CSD appeared at initial omegas >100, where nuclei formed having very large specific surface energies. Between omega values of 28 and 69, the CSDs had transitional shapes between log-normal and Ostwald, indicating incomplete ripening prior to the preservation of their shapes by supply-limited, proportionate growth [Fig. 5 in Kile et al. (2000)].

The Ostwald and transitional CSD shapes were formed in the laboratory where calcite was crystallized by the rapid mixing of concentrated calcium and carbonate solutions (Kile et al. 2000). However, such environmental conditions are rare in nature. The Ostwald shape has been found for garnets in metamorphic rock by Miyazaki (1991). Carlson (1999) objected to this interpretation because the surface energy driving force for the ripening of such large porphyroblasts would be negligible. Carlson correctly reasoned that ripening should not be effective for crystals larger than a fraction of a micrometer. However, as was discussed, the Oswald distributions likely formed from extremely small crystals during and immediately after nucleation. These shapes were then preserved for the garnets during supply-limited, proportionate growth.

An entire sequence of CSD shapes, from Ostwald to transitional to log-normal, has been found on Mars for hematite concretions [Martian blueberries; Figs. 2 and 3 in Eberl (2022)]. Concretion diameters were measured from photographs taken during a traverse by the Opportunity rover. This set of distribution shapes indicates differences in initial relative levels of groundwater supersaturation with respect to hematite solubility [see Fig. 6 in Kile et al. (2000) for analogous calcite experiments]. Concretions likely precipitated from hydrothermal solutions that were generated suddenly by bolide impact on groundwater or permafrost (Eberl 2022). Iron for the hematite may have come from the bolide.

There is another kind of ripening, other than Ostwald, during which crystals dissolve randomly with respect to size, thereby supplying nutrients for other crystals to grow. During such supply-limited random ripening (also termed non-Ostwald ripening), something other than specific surface area influences solubility. For example, some crystals could be less stable due to lattice strain, polytype, or because they are located in hotspots. Assuming that the less stable crystals disappear completely, the initial CSD shape (β^2) remains constant as mean size increases [Fig. 11 in Eberl et al. (1998)], thereby mimicking supply-limited growth, but this process differs because it occurs in a closed system (here defined as a system in which nutrients for growth come from the dissolution of the crystals themselves), and because a large amount of material passes through a solution for a small increase in mean size. It is not known if random ripening is an important growth mechanism in nature because its CSD does not have a distinctive shape of its own. Evidence for such ripening has been noted experimentally in isotopic studies of the growth of Fisher calcite crystals treated hydrothermally in a closed system at 500 °C for various lengths of time [Figs. 18 and 19 in Eberl et al. (1998)].

Mineral CSDs may have other shapes. For example, samples that have undergone several nucleation events can be composed of multiple log-normal distributions [Fig. 2c in Kile et al. (2000)]. These distributions can be decomposed into their component log-normal CSDs by fitting them with appropriate means and variances using Equation 1. In addition, CSD shapes that have undergone mixing or winnowing by sediment transportation can be recognized by the relation between α and β^2, the values for which may lie outside a field expected for in situ crystal growth, as was demonstrated for the mineral illite in Yukon River sediments [Fig. 18b in Eberl (2004)]. In a like manner, the reaction path for illite crystals can be ascertained from their thickness distribution shapes by plotting distribution parameters onto an α vs. β^2 diagram, as was shown for illite crystals from the San Juan Mountains, Colorado [Figs. 6 and 7 in Bove et al. (2002)].

Origin of proportionate growth

CSDs may increase in mean size by proportionate growth or by constant growth (Eberl et al. 2002a). The latter growth law, which is expressed $X_{(j+1)} = X_j + k$, often is assumed in modeling, for example, in population balance modeling (Marsh 1998), in McCabe's ΔL law (McCabe 1929), and in the Avrami equation, also known as the Johnson Mehl Avrami Kolmogorov (JMAK) equation (Shizad and Viney 2023). But, based on evidence from CSD shapes, constant growth is a rarity. Growth experiments with centimeter-size K-alum crystals having various initial sizes indicate that, for such large crystals, proportionate growth occurs in stirred systems, whereas constant growth occurs in systems that are not stirred [Figs. 1 and 2 in Kile and Eberl (2003)]. Thus, the advective supply of nutrients to crystals favors proportionate growth, whereas diffusion in still solutions leads to constant growth. The reason for this behavior is attributed to a nutrient-depleted boundary layer in solution next to a crystal. This layer is progressively thinned by the greater velocity necessary for a solution to contour around larger crystals, thereby tending to increase the growth rate based on crystal diameter, as has been modeled by Stefan-Kharicha et al. (2020).

A contrary result was found during the experimental nucleation and growth of fine (28 μm mean) calcite crystals [Fig. 3 in Kile and Eberl (2003)]. They exhibited proportionate growth by retaining a log-normal CSD for both stirred and unstirred systems,

an effect attributed to their small size and to solution movement during initial mixing or to visually unobserved convection and/or Brownian motion (Kile the al. 2000). However, calcite CSDs showed the narrowing effect expected for constant growth when grown from concentrated solutions in a silica gel-filled column (Kile and Eberl 2003). (Silica gel was used to minimize advection and increase nutrient supply by diffusion.) These calcite crystals grew to a mean diameter of about 310 μm and had a very small variance of 0.02. An initial Ostwald distribution shape and variance ($\beta^2 = 0.07$) was recovered by subtracting a constant 140 μm from each crystal diameter, indicating that constant growth began to alter an Ostwald distribution shape at a mean diameter of about 170 μm [Fig. 4c in Kile and Eberl (2003)].

Two examples of constant growth were discovered in natural flow-restricted environments (Kile et al. 2000). Calcite CSDs within a molar tooth structure (Proterozoic Belt Supergroup, Western Montana, U.S.A.), having a mean size of 13 μm and a variance of 0.02, started constant growth at 7.5 μm from an initial Ostwald distribution shape [Fig. 5 in Kile and Eberl (2003)]. Possible greigite crystals, found in a diatom test in Pyramid Lake, Nevada, also may have undergone some constant growth that deformed an initial Ostwald CSD [Fig. 6 in Kile and Eberl (2003)].

There may be a practical application for these observations. If one wants to create a CSD containing uniform sizes (for example, a non-scoring abrasive or a congruently dissolving drug), one could encourage the initial formation of an Ostwald CSD by nucleation at large supersaturation, followed by constant growth in an immobile solution, which would further decrease variance (Eberl et al. 2002b). It may also be possible to encourage a narrowing of CSDs through rapid stirring or flushing, whereby the flow of solution around crystals is fast enough to be minimally affected by crystal diameters.

Implications

The LPE and the related volume-constrained LPE offer a concise and simple explanation for some of the baffling features concerning crystal growth, including size-dependent growth, crystal growth dispersion, the common log-normal shape, and the narrow range of variance for each of the three basic types of CSDs [Fig. 7 in Kile et al. (2000)]. The equation also indicates that growth depends on the incorporation of nanoparticles rather than single atoms, a prediction that accords with electron micrograph evidence mentioned previously.

A random number lies at the heart of this equation, but what are the consequences of accepting randomness? As was discussed, randomness means that the growth rate of individual crystals cannot be calculated precisely, but only the distribution shape can be predicted.

Analogous to crystal growth, randomness also appears in the foundations of quantum mechanics. The double slit experiment indicates that one cannot calculate (based on the Schrödinger equation) the precise location of an electron fired through double slits onto a fluorescent screen, but one can only predict the shape of the distribution of a large number of electrons striking the screen. Likewise, one cannot predict the moment for the radioactive decay of an individual atom, but only the decay rate for a large group of atoms. Stochastic models also are used to model chemical reactions (Gillespie 2007). In fact, many natural systems likely have such built-in randomness (Mann 1970; Ilyan 2020), especially if they express a log-normal distribution. The presence of a random component means that experimental results are not precisely reproducible, no matter how much care is taken. However, on the positive side, the presence of randomness frees us from a completely deterministic worldview.

Acknowledgments

I thank Manny Knill and Lynda Williams for their substantial comments on the initial manuscript. I also thank my former coauthors, especially Dan Kile, for his excellent experimental work. Thanks also to Alain Baronnet, who introduced the author to the science of CSDs during a lecture in Paris many years ago. I apologize to scientists who were misled by mistaken notions concerning crystal growth published in Eberl and Środoń (1988) and Eberl et al. (1990). I acknowledge pioneering papers on the use of CSDs in geology by Marsh (1988), Cashman and Ferry (1988), and Cashman and Marsh (1988), papers that were partly based on investigations of crystal growth in continuous-flow industrial crystallizers by Randolph and Larson (1971). Such geological studies draw conclusions from log-linear plots of CSDs and generally assume a constant growth rate, whereas the present paper simulates the shapes of CSDs from crystal growth mechanisms. I am deeply grateful to the U.S. Geological Survey for its support of this research prior to my retirement.

References cited

Badino, G.V., Ferreira, A., Forti, P., Giovani, P., Giulivo, I., Infante, G., Lo Mastro, F., Sanna, L., and Tedeschi, R. (2009) The Naica caves survey. Fifteenth International Congress of Speleology At: Kerrville, Texas (U.S.A.), 1764–1769.

Bove, D.J., Eberl, D.D., McCarty, D.K., and Meeker, G.P. (2002) Characterization and modeling of illite crystal particles and growth mechanisms in a zoned hydrothermal deposit, Lake City, Colorado. American Mineralogist, 87, 1546–1556, https://doi.org/10.2138/am-2002-11-1204.

Carlson, W. (1999) The case against Ostwald ripening of porphyroblasts. Canadian Mineralogist, 37, 403–413.

Cashman, K.V. and Ferry, J.M. (1988) Crystal size distribution (CSD) in rocks and the kinetics and dynamics of crystallization. Metamorphic crystallization. Contributions to Mineralogy and Petrology, 99, 401–415, https://doi.org/10.1007/BF00371933.

Cashman, K.V. and Marsh, B.D. (1988) Crystal size distribution (CSD) in rocks and the kinetics and dynamics of crystallization ii. Makaopuhi lava lake. Contributions to Mineralogy and Petrology, 99, 292–305, https://doi.org/10.1007/BF00375363.

De Yoreo, J.J., Gilbert, P.U.P.A., Sommerdijk, N.A.J.M., Penn, R.L., Whitelam, S., Joester, D., Zhang, H., Rimer, J.D., Navrotsky, A., Banfield, J.F., and others. (2015) Crystallization by particle attachment in synthetic, biogenic, and geologic environments. Science, 349, print extended abstract at p. 498, online aaa6760 https://doi.org/10.1126/science.aaa6760.

Eberl, D.D. (2004) Quantitative mineralogy of the Yukon River system: Changes with reach and season, and determining sediment provenance. American Mineralogist, 89, 1784–1794, https://doi.org/10.2138/am-2004-11-1225.

——— (2022) On the formation of Martian blueberries. American Mineralogist, 107, 153–155, https://doi.org/10.2138/am-2022-8167.

Eberl, D.D. and Środoń, J. (1988) Ostwald ripening and interparticle-diffraction effects for illite crystals. American Mineralogist, 73, 1335–1345.

Eberl, D.D., Środoń, J., Kralik, M., Taylor, B.E., and Peterman, Z.E. (1990) Ostwald ripening of clays and metamorphic minerals. Science, 248, 474–477, https://doi.org/10.1126/science.248.4954.474.

Eberl, D.D., Drits, V.A., and Środoń, J. (1998) Deducing growth mechanisms for minerals from the shapes of crystal size distributions. American Journal of Science, 298, 499–533, https://doi.org/10.2475/ajs.298.6.499.

——— (2000) User's Guide to GALOPER: a program for simulating the shapes of crystal size distributions—and associated programs. U.S. Geological Survey Open-File Report., OF 00-505.

Eberl, D.D., Kile, D.E., and Drits, V.A. (2002a) On geological interpretations of crystal size distributions: Constant vs. proportionate growth. American Mineralogist, 87, 1235–1241, https://doi.org/10.2138/am-2002-8-923.

Eberl, D.D., Kile, D.E., and Hoch, A.R. (2002b) Crystallization of powders having uniform particle sizes by Ostwald ripening at large levels of supersaturation. U.S. Patent 6,379,459, April 30, 2002.

Gillespie, D.T. (2007) Stochastic simulation of chemical kinetics. Annual Review of Physical Chemistry, 58, 35–55, https://doi.org/10.1146/annurev.physchem.58.032806.104637.

Ilan, Y. (2020) Order through disorder: the characteristic variability of systems. Frontiers in Cell Development Biology, 8, 1–12, https://doi.org/10.3389/fcell.2020.00186.

Ivanov, V.K., Fedorov, P.P., Baranchikov, A.Y., and Osiko, V.V. (2014) Oriented attachment of particles: 100 years of investigations of non-classical crystal growth. Russian Chemical Reviews, 83, 1204–1222, https://doi.org/10.1070/

RCR4453.
Kile, D.E. and Eberl, D.D. (1999) Crystal growth mechanisms in miarolitic cavities in the Lake George ring and vicinity, Colorado. American Mineralogist, 84, 718–724.
——— (2003) On the origin of size-dependent and size-independent crystal growth: Influence of advection and diffusion. American Mineralogist, 88, 1514–1521, https://doi.org/10.2138/am-2003-1014.
Kile, D.E., Eberl, D.D., Hoch, A.R., and Reddy, M.M. (2000) An assessment of calcite crystal growth mechanisms based on crystal size distributions. Geochimica et Cosmochimica Acta, 64, 2937–2950, https://doi.org/10.1016/S0016-7037(00)00394-X.
Koch, A.L. (1966) The logarithm in biology. 1. Mechanisms generating the log-normal distribution exactly. Journal of Theoretical Biology, 12, 276–290, https://doi.org/10.1016/0022-5193(66)90119-6.
Lifshitz, I.M. and Slyozov, V.V. (1961) The kinetics of precipitation from supersaturated solid solutions. Journal of Physics and Chemistry of Solids, 19, 35–50, https://doi.org/10.1016/0022-3697(61)90054-3.
Mann, C.J. (1970) Randomness in nature. Geological Society of America Bulletin, 81, 95–104, https://doi.org/10.1130/0016-7606(1970)81[95:RIN]2.0.CO;2.
Markworth, A.J. (1970) The kinetic behavior of precipitate particles under Ostwald ripening conditions. Metallography, 3, 197–208, https://doi.org/10.1016/0026-0800(70)90029-7.
Marsh, B.D. (1988) Crystal size distribution (CSD) in rocks and the kinetics and dynamics of crystallization. 1. Theory. Contributions to Mineralogy and Petrology, 99, 277–291, https://doi.org/10.1007/BF00375362.
——— (1998) On the interpretation of crystal size distributions in magmatic systems. Journal of Petrology, 39, 553–599.
McCabe, W.L. (1929) Crystal growth in aqueous solutions. Industrial Engineering Progress, 21, 30–33.
Miyazaki, K. (1991) Ostwald ripening of garnet in high *P*/*T* metamorphic rocks. Contributions to Mineralogy and Petrology, 108, 118–128, https://doi.org/10.1007/BF00307331.
Randolph, A.D. and Larson, M.A. (1971) Theory of Particulate Processes: Analysis and Techniques of Continuous Crystallization, 1st ed., 268 p. Academic Press.
Shizad, K. and Viney, C. (2023) A critical review on applications of the Avrami equation beyond materials science. Journal of the Royal Society Interface, 20, https://doi.org/10.1098/rsif2023.0242.
Stefan-Kharicha, M., Kharicha, A., Zaidat, K., Reiss, G., Eßl, W., Goodwin, F., Wu, M., Ludwig, A., and Mugraue, C. (2020) Impact of hydrodynamics on growth and morphology of faceted crystals. Journal of Crystal Growth, 541, 1–11, https://doi.org/10.1016/j.jcrysgro.2020.125667.
Wagner, C. (1961) Theorie der alterung von niederschlägen durch umlösen (Ostwald reifung). Zeitschrift für Elektrochemie, 65, 581–591, https://doi.org/10.1002/bbpc.19610650704 (in German).

Manuscript received October 24, 2022
Manuscript accepted March 17, 2023
Accepted manuscript online March 23, 2023
Manuscript handled by Daniel Hummer

Endnote:

[1]Deposit item AM-24-18851. Online Materials are free to all readers. Go online, via the table of contents or article view, and find the tab or link for supplemental materials.